

Leidenfrost droplets trampoline

Dongdong Liu^{ab} and Tuan Tran^{ab*}

^a*School of Mechanical&Aerospace Engineering, Nanyang Technological University, 50 Nanyang Avenue, 639798, Singapore.* ^b*HP-NTU Digital Manufacturing Corporate Lab, Nanyang Technological University, 50 Nanyang Avenue, 639798 Singapore.*

(Dated: January 7, 2022)

A liquid droplet hovering on a hot surface is commonly referred to as a Leidenfrost droplet. In this study, we discover that a Leidenfrost droplet involuntarily performs a series of distinct oscillations as it shrinks during the span of its life. The oscillation first starts out erratically, followed by a stage with stable frequencies, and finally turns into periodic bouncing with signatures of a parametric oscillation and occasional resonances. The last bouncing stage exhibits nearly perfect collisions. We showed experimentally and theoretically the enabling effects of each oscillation mode and how the droplet switches between such modes. We finally show that these self-regulating oscillation modes and the conditions for transitioning between modes are universal for all tested combinations of liquids and surfaces.

Leidenfrost effect, a two-century old phenomenon [1, 2] causing levitation of liquid droplets deposited on hot surfaces, has been playing a critical role in an increasing number of modern technologies. As the effect completely removes liquid-solid contact and subsequently liberates the liquid from frictional constraint of the surrounding, it has great potential to transform liquid-transport applications ranging from largescale drag reduction [3], rapid and autonomous transport of liquid droplets [4, 5], to nanoscale manufacturing processes [6]. Our current understanding of the Leidenfrost phenomenon is largely based on the steady-state assumption, an approach used to justify exclusion of minute but accumulative effects such as drop size reduction by evaporation. The resulting analysis, while offers tremendous insights into the short-time Leidenfrost dynamics, filters out phenomena only visible at longer timescales, e.g., the life time of Leidenfrost droplets.

Here, we reveal that as a Leidenfrost droplet shrinks, it involuntarily performs a series of trampolining motions, starting erratically at the beginning, followed by regular oscillation and finally settling at periodic bouncing towards the end of its life time. The bouncing behavior has an unusually high restitution coefficient and exhibits signatures of parametric oscillation with occasional resonances. Our findings demonstrate the active nature of Leidenfrost droplets at long timescales by showing that they exhibit self-regulating ability by switching through different modes of oscillation in response to reduction in drop size by evaporation. The underlying active mechanism may serve as a basis to explore strategies for energy harvesting or frictionless and autonomous liquid transport.

The spontaneous trampolining motion, of a Leidenfrost droplet is self-triggered and occurs as the droplet loses its weight to evaporation. The transitions between characteristic behaviors inevitably result from liquid evapora-

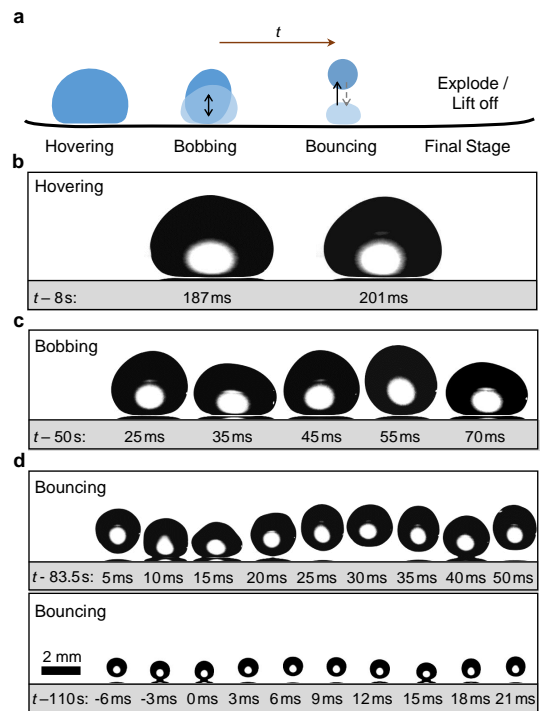


FIG. 1. (a) Schematic illustrating the characteristic behaviors of a Leidenfrost droplet as it evaporates and shrinks. The initial drop size typically is larger than the liquid’s capillary length. Once deposited on a superheated surface the droplet goes through the following stages: (b) hovering (c) bobbing and (d) bouncing. Eventually, when the drop becomes sufficiently small, it reaches the final stage in which it either lifts off or explodes [7, 8]. The snapshots from panels (b) to (d) were taken from an experiment using DI water as the working fluid. The surface was polished aluminum surface and heated to 380 °C.

tion and subsequent size reduction, from the liquid’s capillary length (several millimeters) to hundreds of micrometers. In considering the underlying phenomena, in particular the droplet’s vertical motion, we trap Leidenfrost droplets horizontally by using a slightly curved smooth surface, thereby minimizing the Leidenfrost wheeling ef-

* ttran@ntu.edu.sg

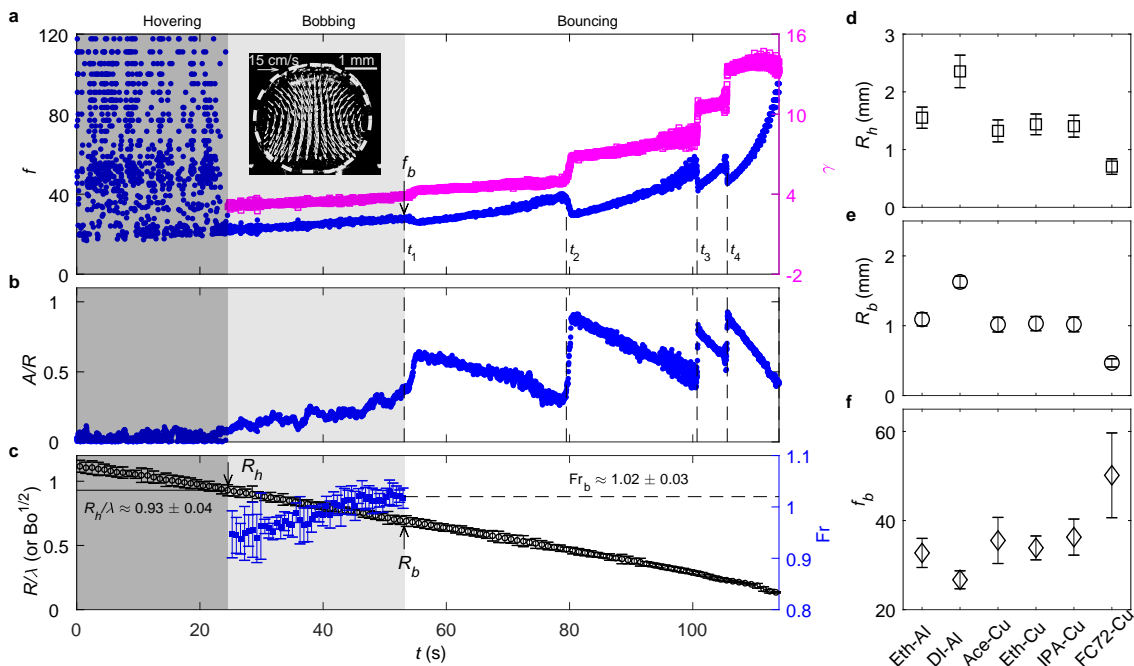


FIG. 2. (a) Representative plot showing the oscillation frequency f (left axis) and the ratio $\gamma = 2f_n/f$ (right axis) versus time t as the droplet transitions through several characteristic stages: hovering, bobbing and bouncing. Parametric resonance occurs in the bouncing stage at t_1 , t_2 , t_3 and t_4 . Inset: Internal velocity field of a droplet in the bobbing stage. (b) Dimensionless oscillation amplitude A/R versus time t . (c) Dimensionless radius $R/\lambda = \text{Bo}^{1/2}$ (left axis) and Froude number Fr in the bobbing stage (right axis) versus t . The solid line indicates that the transition from hovering to bobbing stage happens at $R/\lambda \approx 0.93$, or equivalently $\text{Bo} \approx 0.86$. The dashed line indicates that the transition from bobbing to bouncing occurs at $\text{Fr} \approx 1.0$. Variation in (d) droplet radius R_h at the hovering-bobbing transition (e) droplet radius R_b and (f) frequency f_b at the bobbing-bouncing transition for various fluid-surface combinations. The tested fluids are ethanol (Eth), DI water (DI), acetone (Ace), IPA and FC72. The tested surface materials are copper (Cu) and aluminum (Al).

fect [9] that triggers the horizontal motion.

During the lifetime of a Leidenfrost droplet, its behavior transitions through several stages, as illustrated in the schematic shown in Fig. 1a. A droplet larger than the liquid's capillary length after deposited on a sufficiently heated surface first hovers around on its own vapor layer. In this so-called *hovering* stage (Fig. 1b), the droplet has a relatively large flatten area at the bottom due to gravity and this area does not vary significantly with time. As the droplet gets smaller due to evaporation, capillary force becomes dominating over gravitational force, causing its behavior transition from hovering to *bobbing*, i.e., periodic vertical deformation without leaving the surface (Fig. 1c). When the droplet radius reduces to a critical value, it starts *bouncing* on the surface, i.e., the droplet is no longer separated from the surface by a thin vapor film but jumps up and down periodically. (Fig. 1d). Once the droplet becomes sufficiently small ($R \sim 100 \mu\text{m}$), it either takes a final leap out of the camera's view or explodes [7, 8].

The recorded phenomenological behaviors of Leidenfrost droplets are robust for all tested liquids, including deionized (DI) water, ethanol, isopropyl alcohol (IPA), acetone and FC-72, as well as for surface materials such as copper and aluminum [10]. We also verify these behaviors for a wide range of surface temperature, from 180 °C

to 440 °C, confirming that the phenomena are not material and temperature specific.

To shed light into the observed transient dynamics of Leidenfrost droplets, we track the vertical position y_c of the center of mass as a function of time. Subsequently, the frequency f and amplitude A of the periodic motion of the center of mass can be extracted. In Fig. 2a and b, we show representative plots of f and the normalized amplitude A/R for a DI water droplet on a aluminum surface at 380 °C. Here R is the droplet radius calculated by assuming a spherical droplet of the same volume with the one recorded from the side view [11]. The frequency plot presents a clear picture of the transition from the hovering stage, where large scattering in f is observed, to the bobbing stage, where f gently increases with time.

The erratic oscillation of the droplet in the hovering stage originates from capillary waves on its surface. Indeed, the droplet radius measured in this stage is larger than the capillary length $\lambda = (\sigma/\rho g)^{1/2}$ (see Fig. 2c). Here, ρ and σ respectively are the density and surface tension at the liquid's boiling point [9, 12]. As the droplet radius becomes smaller than λ the capillary waves diminish, giving rise to more regular oscillations. As a result, we conclude that the transition from hovering to bobbing occurs when $R \approx \lambda$, or equivalently when the Bond number $\text{Bo} = \rho g R^2 / \sigma = (R/\lambda)^2 \approx 1$.

We now focus on the transition from bobbing to bouncing. Although not clearly displayed through f , this transition is clearly determined from the recording when the droplet starts jumping readily from the surface. We observe experimentally that the internal flow of a droplet in the bobbing stage resembles a toroidal field, i.e., a strong downward flow at the center of the droplet (Fig. 2a, inset) [13]. This flow field provides a crucial evidence indicating the driving mechanism of the droplet's oscillation and the eventual transition to bouncing: the temperature difference between the bottom and top of the droplet generates a thermocapillary effect that induces the internal flow, the associated pressure difference inside the droplet, and subsequently its surface deformation. As the droplet radius continuously decreases, the involving parameters of oscillation, i.e., the frequency associated with the internal flow and the droplet's natural frequency, also vary with time, although at different rates [14]. This eventually leads the oscillating droplet to parametric resonances and the observed abrupt growths in its amplitude (Fig. 2b). The transition to bouncing therefore occurs when the excited oscillation gains sufficient upward acceleration to overcome gravity. If we denote V_i the characteristic velocity of internal flow, then the acceleration associated with the internal flow ($a = V_i^2/2R$) in comparison with the gravitational acceleration is evaluated by the Froude number $\text{Fr} = (a/g)^{1/2} = V_i/(2Rg)^{1/2}$. In other words, the droplet overcomes gravity when $\text{Fr} \gtrsim 1$.

To test the hypothesis that the transition from bobbing to bouncing is possible at $\text{Fr} \approx 1$, we now examine the dependence of the Froude number on the internal flow characteristics, in particular its frequency f_i . Since the oscillation is driven by the internal flow and recall that f is the oscillation frequency of the droplet, we have $f \approx f_i \approx V_i/4R$, giving $V_i \approx 4Rf$. By substituting the expression of V_i into the one for Fr and using the natural frequency f_n of the droplet to normalize f , we obtain the following expression for Fr :

$$\text{Fr} \approx \left(\frac{6}{\pi}\right)^{1/2} \frac{f}{f_n} \left(\frac{R}{\lambda}\right)^{-1}. \quad (1)$$

Here, $f_n = (\sigma/m)^{1/2}$, where $m = (4\pi/3)\rho R^3$ is the mass of the droplet [15–17]. In Fig. 2c, we show how Fr changes in the bobbing stage. Indeed, the condition $\text{Fr} \approx 1$ holds at the transition to bouncing, indicating that the upward acceleration caused by internal flows overcomes the gravitational acceleration at the transition from bobbing to bouncing.

The two transitions that we observed, therefore, can be understood using the dimensionless numbers Bo and Fr . The first transition occurs when $\text{Bo} \approx 1$ and the second transition occurs when $\text{Fr} \approx 1$. We confirm experimentally that although different fluid–surface combinations yield disparate values for the radius R_h at the hovering–bobbing transition, the radius R_b , or the frequency f_b at the bobbing–bouncing transition (Fig. 2d–f) [18], the conditions for transitions always hold, as shown in Fig. 3a.

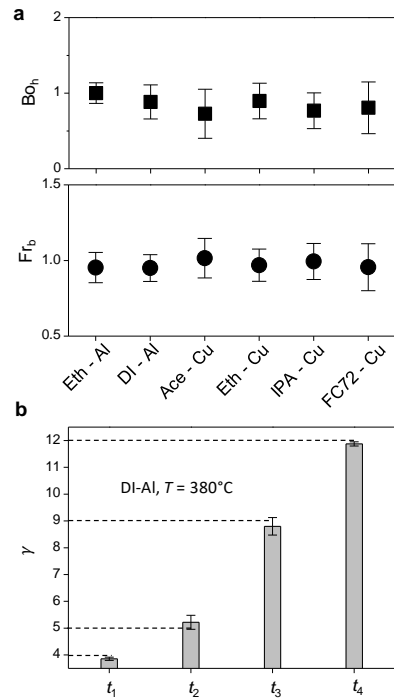


FIG. 3. (a) Plots showing the Bond number Bo_h at the hovering–bobbing transition and the Froude number Fr_b at the bobbing–bouncing transition for various fluid–surface combinations. (b) Plot showing the ratio $\gamma = 2f_n/f$ evaluated at the time of resonances. Dashed lines indicate integer values of γ .

We now focus on the bouncing stage to discuss the abrupt drops in f and the corresponding jumps in A (Fig. 2a and b). We note that an increasing natural frequency of the droplet, combined with the sudden drops in its frequency f at t_1, t_2, t_3 and t_4 (Fig. 2a) indicates that the droplet may experience parametric resonances at such moments [19, 20]. Indeed, if we follow the signature of parametric resonances and examine the ratio $\gamma = 2f_n/f$, we observe that γ increases substantially, from 2.8 at the bobbing–bouncing transition to 14.7 at the end of the bouncing stage. Whenever there is a sudden drop in f , i.e., at $t_1, t_2, t_3,$ or t_4 , the corresponding value of γ is approximately at the vicinity of an integer (see Fig. 3b). The first resonance at t_1 allows the droplet to gain sufficient upward acceleration to overcome gravitational acceleration and transition to the bouncing stage. As a result, we conclude that the sudden decreases in f and the corresponding amplitude jumps in the bouncing stage result from the droplet going through parametric resonances [22].

Between resonances, the parametric oscillation of a bouncing droplet, affected by its internal flow, is accompanied by a remarkable high *contact time* [23] with the heated surface. Here, we define the contact time t_c of each bouncing period using the duration in which the droplet appears in contact with the surface (see Fig. 4a), although strictly speaking, a Leidenfrost droplet and the

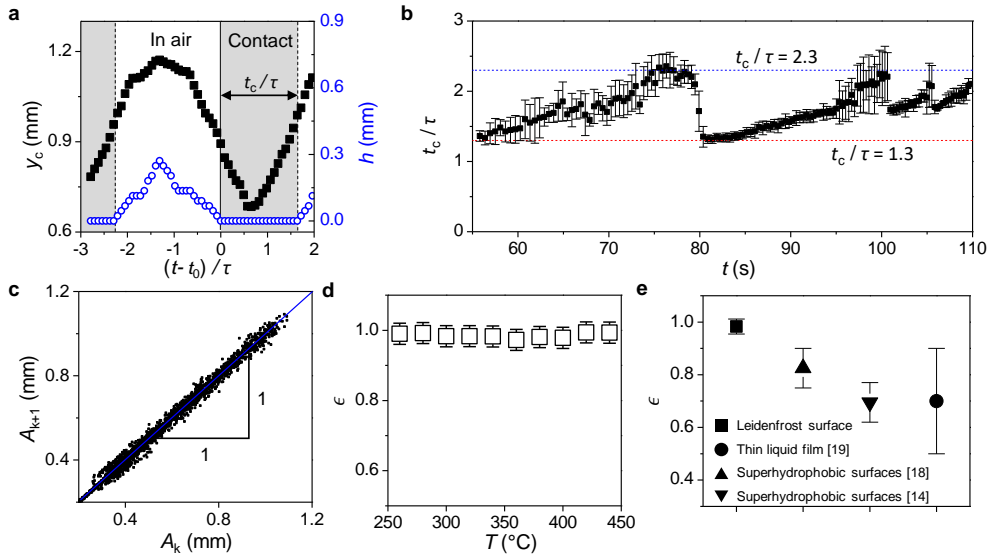


FIG. 4. (a) Representative plots showing the vertical centre of mass y_c (left axis, square markers) and the gap h between the droplet and the surface (right axis, circular markers) versus the dimensionless time $(t-t_0)/\tau$ in the bouncing stage. The shaded area indicates the contact time t_c during which the droplet contacts with the surface ($h \approx 0$). (b) Dimensionless contact time t_c/τ versus t in bouncing stage. The dash lines represent the lower and upper bounds of t_c/τ . (c) Amplitude ratio A_{k+1}/A_k of two consecutive oscillations at any cycle k in the bouncing stage. (d) Restitution coefficient ϵ averaged over the entire bouncing stage of a water droplet versus wall temperature T . (e) Comparison of restitution coefficient ϵ of water droplets on different surfaces: Leidenfrost surface (present study - squares), thin liquid film (circles), superhydrophobic surfaces (upward- and downward- triangles).

heated surface are always separated by a vapor layer. In Fig. 4b, we show the variation of the normalized contact time t_c/τ in the bouncing stage, with $\tau = 1/f_n$ being the natural bouncing period. The plot shows that t_c/τ varies between 1.3 and 2.3, and is mostly higher than that in the case of impacting droplet on unheated surface, where $t_c/\tau \approx 1.3$ [17, 21]. The longer contact time for bouncing Leidenfrost droplets may allow the thermocapillary-induced flow to energize the droplet, resulting in higher stored surface energy and subsequently an unusually high recovery of gravitational potential of the bouncing motion. This is best illustrated by examining the relation between the amplitude A_{k+1} of bouncing cycle $k+1$ and that of the immediately preceding cycle, A_k . As shown in Fig. 4c, the amplitudes A_k and A_{k+1} of any two consecutive cycles are always almost identical, indicating that the restitution coefficient $\epsilon_k = (A_{k+1}/A_k)^{1/2}$ of any cycle k is approximately unity. The average restitution coefficient ϵ for the entire bouncing stage, shown in Fig. 4c, ranges from 0.97 to 0.99 with the surface temperature varying from 300°C to 440°C. This is remarkably higher than the restitution coefficient of droplets impinging on superhydrophobic surfaces ($0.5 \leq \epsilon \leq 0.9$) [17, 24], or that on thin liquid films ($0.75 \leq \epsilon \leq 0.9$) [25] (see Fig. 4e). We note that $\epsilon \approx 1$ suggests that the energy lost to viscous dissipation is almost completely compensated by the kinetic energy gained by the thermocapillary-induced flow. The fact that ϵ is independent of temperature highlights a distinctive feature of thermocapillary stress: the liquid temperature at the droplet's bottom surface remains approximately fixed at boiling temperature, leading to a

stable vertical temperature difference across the droplet and subsequently a thermocapillary stress that depends weakly on the temperature of the solid surface.

Leidenfrost droplets, therefore, always set off to a series of trampolining motions with a variety of rhythms. A sufficiently large Leidenfrost droplet always starts hovering on the heated surface with fluctuating frequencies until its size becomes comparable to the liquid's capillary length, at which the droplet starts bobbing, i.e., oscillating with more regular frequencies but without bouncing. A transition from bobbing to bouncing occurs when the Froude number becomes larger than unity, signifying that the upward acceleration caused by internal flows overcomes the gravitational acceleration. In the bouncing stage, the droplet's dynamics are driven by parametric oscillation with occasional resonances whereby the oscillation frequency drops and the amplitude trebles. The bouncing motions of the Leidenfrost droplet is also characterized by an unusually high restitution coefficient resulted from the thermocapillary-induced flow compensating the lost energy due to viscosity. Our findings of the spontaneous trampolining motions of Leidenfrost droplets complete their portraiture as an active system capable of creating its own motions and energetic states. The underlying active mechanism may provide a promising avenue for frictionless liquid manipulation and transport, as well as a potential strategy for energy harvesting.

This research was conducted in collaboration with HP Inc. and supported by Nanyang Technological University and the Singapore Government through the Industry Alignment Fund-Industry Collaboration Projects Grant.

-
- [1] J. G. Leidenfrost, *Int. J. Heat Mass Transf.* **9**, 1153 (1966).
- [2] D. Quéré, *Annu. Rev. Fluid Mech.* **45**, 197 (2013).
- [3] I. U. Vakarelski, J. D. Berry, D. Y. C. Chan, and S. T. Thoroddsen, *Phys. Rev. Lett.* **117**, 114503 (2016).
- [4] H. Linke, B. J. Alemán, L. D. Melling, M. J. Taormina, M. J. Francis, C. C. Dow-Hygelund, V. Narayanan, R. P. Taylor, and A. Stout, *Phys. Rev. Lett.* **96**, 154502 (2006).
- [5] J. Li, Y. Hou, Y. Liu, C. Hao, M. Li, M. K. Chaudhury, S. Yao, and Z. Wang, *Nat. Phys.* **12**, 606 (2016).
- [6] J. Cordeiro and S. Desai, *ASME. J. Micro. Nano-Manuf.* **4**, 041001 (2016).
- [7] F. Celestini, T. Frisch, and Y. Pomeau, *Phys. Rev. Lett.* **109**, 034501 (2012).
- [8] S. Lyu, V. Mathai, Y. Wang, B. Sobac, P. Colinet, D. Lohse, and C. Sun, *Sci. Adv.* **5**, eaav8081 (2019).
- [9] A. Bouillant, T. Mouterde, P. Bourriane, A. Lagarde, C. Clanet, and D. Quéré, *Nat. Phys.* **14**, 1188 (2018).
- [10] See Supplementary Material, section I for oscillation characteristics of tested liquids.
- [11] See Supplementary Material, section II for variation of Bond number with time.
- [12] A.-L. Biance, C. Clanet, and D. Quéré, *Phys. Fluids* **15**, 1632 (2003).
- [13] See Supplementary Material, section III for the internal flow field obtained using PIV.
- [14] See Supplementary Material, section IV for how the frequency changes with time.
- [15] J. Moláček and J. W. Bush, *J. Fluid Mech.* **727**, 582 (2013).
- [16] T. Gilet and J. W. Bush, *J. Fluid Mech.* **625**, 167 (2009).
- [17] T. M. Schutzius, S. Jung, T. Maitra, G. Graeber, M. Köhme, and D. Poulikakos, *Nature* **527**, 82 (2015).
- [18] See Supplementary Material, section V for the effect of surface temperature on the transitions.
- [19] L. D. Landau and E. Lifshitz, *Theoretical Physics. Vol. 1 Mechanics.* (Moscow, Nauka, 1976).
- [20] R. A. Ibrahim, *Parametric random vibration.* (Courier Dover Publications, 2008).
- [21] D. Richard, C. Clanet, and D. Quéré, *Nature* **417**, 811 (2002).
- [22] See Supplementary Material, section VI for more information on parametric resonances.
- [23] J. C. Bird, R. Dhiman, H.-M. Kwon, and K. K. Varanasi, *Nature* **503**, 385 (2013).
- [24] D. Richard and D. Quéré, *Eur Phys. Lett.* **50**, 769 (2000).
- [25] C. Hao, J. Li, Y. Liu, X. Zhou, Y. Liu, R. Liu, L. Che, W. Zhou, D. Sun, L. Li, *et al.*, *Nat. commun.* **6**, 7986 (2015).